AEM
Journals.ASM.org

Overexpression of *fetA* (*ybbL*) and *fetB* (*ybbM*), Encoding an Iron Exporter, Enhances Resistance to Oxidative Stress in *Escherichia coli*

Sergios A. Nicolaou,[a] Alan G. Fast,[a] Eiko Nakamaru-Ogiso,[b] Eleftherios T. Papoutsakis[a]

Department of Chemical and Biomolecular Engineering, University of Delaware, Newark, Delaware, USA[a]; Department of Biochemistry and Biophysics, School of Medicine, University of Pennsylvania, Philadelphia, Pennsylvania, USA[b]

Reactive oxygen species are generated by redox reactions and the Fenton reaction of H_2O_2 and iron that generates the hydroxyl radical that causes severe DNA, protein, and lipid damage. We screened *Escherichia coli* genomic libraries to identify a fragment, containing *cueR*, *ybbJ*, *qmcA*, *ybbL*, and *ybbM*, which enhanced resistance to H_2O_2 stress. We report that the Δ*ybbL* and Δ*ybbM* strains are more susceptible to H_2O_2 stress than the parent strain and that *ybbL* and *ybbM* overexpression overcomes H_2O_2 sensitivity. The *ybbL* and *ybbM* genes are predicted to code for an ATP-binding cassette metal transporter, and we demonstrate that YbbM is a membrane protein. We investigated various metals to identify iron as the likely substrate of this transporter. We propose the gene names *fetA* and *fetB* (for Fe transport) and the gene product names FetA and FetB. FetAB allows for increased resistance to oxidative stress in the presence of iron, revealing a role in iron homeostasis. We show that iron overload coupled with H_2O_2 stress is abrogated by *fetA* and *fetB* overexpression in the parent strain and in the Δ*fur* strain, where iron uptake is deregulated. Furthermore, we utilized whole-cell electron paramagnetic resonance to show that intracellular iron levels in the Δ*fur* strain are decreased by 37% by *fetA* and *fetB* overexpression. Combined, these findings show that *fetA* and *fetB* encode an iron exporter that has a role in enhancing resistance to H_2O_2-mediated oxidative stress and can minimize oxidative stress under conditions of iron overload and suggest that FetAB facilitates iron homeostasis to decrease oxidative stress.

Resistance to oxidative stress is important in the ability of bacteria to deal with several important milieus: oxidative stress encountered during cellular immune responses against bacteria (oxidative burst by macrophages and neutrophils) (1, 2); oxidative stress in the environment due to changing oxygen concentrations (3), toxic chemicals, and metal ions (4–7); and oxidative stress in bioprocessing (8, 9). Reactive oxygen species (ROS), which include superoxide (O_2^-), hydrogen peroxide (H_2O_2), and hydroxyl ion (OH^-), are produced during aerobic growth due to the autoxidation of enzymes by redox reactions, by phagosomal NADPH oxidases, by the ferrous iron Fenton reaction ($Fe^{2+} + H_2O_2 \rightarrow Fe^{3+} + OH^- + \cdot OH$), or by copper that can displace iron in iron-sulfur clusters, resulting in cellular damage (2, 6, 10). ROS species readily diffuse through cellular membranes, resulting in protein and DNA damage; thus, cells have developed defenses against oxidative stress. Cellular responses against ROS include the scavenging of reactive species via peroxidases and superoxide dismutases, the sequestration and storage of free unincorporated iron by proteins (ferritins, Dps, and bacterioferritins) (4, 11), the increased import of manganese by MntH against H_2O_2 stress, and the repression of iron import by the iron regulator Fur (2).

Iron metabolism is essential for most organisms (4). To facilitate ferric iron import into the cytoplasm, *Escherichia coli* utilizes ferric chelators (siderophores) to bind the poorly soluble ferric iron and translocate iron into the cytoplasm using ATP (12). Soluble ferrous iron is directly transported by the Feo iron transport system in *E. coli*, encoded by the *feoAB* genes (4, 13). Iron is essential for cell function, but it can be toxic to cells via ROS formation, thus requiring tight regulation. The ferric uptake regulator protein (Fur) controls the expression of genes involved in iron transport (14), but it is also involved in the response to oxidative stress through the regulation of superoxide dismutase genes, which, as stated above, protect against ROS (4).

Siderophores and their receptors have been implicated in pathogenesis (15, 16), and iron chelators are used as therapeutic agents against pathogens (17). ATP-binding cassette (ABC) transporters, including iron siderophores, are also involved in pathogenesis (18) and have a role in oxidative stress. The MtsABC transporter in *Streptococcus pyogenes* was shown to have a role in manganese and iron uptake, and since superoxide dismutases require Mn or Fe as a cofactor, the *mtsABC* mutant was shown to have reduced superoxide dismutase activity and higher susceptibility to oxidative stress (19). Similarly, a SitABCD homologue was shown to facilitate manganese and iron transport in *E. coli* and increase resistance to H_2O_2 (20). Thus, oxidative stress, iron metabolism, and ABC transporters are important in bacterial pathogenesis and functionality.

Despite their role in pathogenesis, cellular maintenance, and the oxidative stress response, metal efflux transporters have not been widely examined, and few are known, such as CopA, which mediates copper efflux (21), and ZntA, which facilitates zinc and cadmium transport (22). Although many transporters facilitate iron import in *E. coli* (4), there is only one known putative iron exporter, FieF, which belongs to the cation diffusion facilitator family (CDF) (23). Since iron is so tightly regulated, with uptake being an important cellular need and cells aiming to maintain an optimum concentration and minimize oxidative stress, it is logical that there should exist exporters to alleviate iron overload and

Received 12 July 2013 **Accepted** 7 September 2013
Published ahead of print 13 September 2013
Address correspondence to Eleftherios T. Papoutsakis, epaps@udel.edu.
Supplemental material for this article may be found at http://dx.doi.org/10.1128/AEM.02322-13.

doi:10.1128/AEM.02322-13

minimize the risk of ROS formation and damage (24). However, such transporters in *E. coli* have been elusive.

We aimed to identify novel genetic determinants of resistance to oxidative stress in *E. coli* using an agnostic approach based on screening of genomic libraries to identify interacting genetic loci in generating tolerant cells (25, 26). This approach led to the identification of the genetic locus comprised of *cueR*, *ybbJ*, *qmcA*, *ybbL*, and *ybbM*, which enhanced tolerance to oxidative stress. We investigated the genes included in this locus, and here we report evidence that overexpression of *ybbL* and *ybbM* increases resistance to H_2O_2-mediated stress. Bioinformatic analysis suggests that these genes encode an uncharacterized ABC transporter system that has a role in metal resistance. We generated a green fluorescent protein (GFP) fusion with YbbM and showed that it is a membrane protein, as predicted. To better understand the mechanism by which these genes increase resistance to oxidative stress, we investigated various metals and show that *ybbL* and *ybbM* can alleviate iron overload coupled with H_2O_2 stress. Therefore, we propose the names *fetA* and *fetB* for the genes. We hypothesized that the FetAB transporter allows for iron export, thus minimizing the formation of ROS by H_2O_2. We demonstrated that *fetA* and *fetB* overexpression in the Δ*fur* mutant results in less intracellular iron, as determined by electron paramagnetic resonance (EPR). The results thus support a mechanism in which this ABC transporter exports iron and minimizes ROS species formation by H_2O_2, although other mechanisms are possible. Further work is required to elucidate the exact mechanism of *fetA* and *fetB*, but our findings provide strong evidence that these genes have a role in enhancing H_2O_2 stress tolerance and are important in the defense against oxidative stress.

MATERIALS AND METHODS

Bacterial strains, plasmids, and growth conditions. Strains and plasmids used in this study are described in Table 1. The plasmid genomic libraries utilized in this study were previously constructed (25). The libraries were methylated in NEB 5-alpha competent *E. coli* cells (New England BioLabs, Ipswich, MA, USA) and were transformed into *E. coli* K-12 strain MG1655 to obtain 2.6×10^8 clones with both plasmid libraries.

E. coli strain BW25113 and the BW25113 Δ*cueR*, BW25113 Δ*qmcA*, BW25113 Δ*fetA* (Δ*ybbL*), and BW25113 Δ*fetB* (Δ*ybbM*) mutants were obtained from the *E. coli* genetic resources at Yale Coli Genetic Stock Center (CGSC) and are part of the Keio Collection of strains (27) (Table 1). The BW25113 Δ*ybbJ* and BW25113 Δ*fur* strains were constructed by using the method of Datsenko and Wanner (28), with primers listed in Table 1 and plasmid pKD4 for amplification of the recombination cassette. pKD46 was used as the helper plasmid for the recombination reaction (28). The BW25113 Δ*fur* Δ*fetB* strain was constructed by eliminating the kanamycin resistance of the BW25113 Δ*fetB* strain with pCP20 (28) and then using Fur primers (Table 1).

E. coli strains were grown in Luria-Bertani (LB) broth or minimal M9 medium with thiamine (10 μg/ml) (29) at 37°C and supplemented with 100 μg/ml ampicillin or 10 μg/ml tetracycline, as required. The optical density at 600 nm (OD_{600}) was determined with a Beckman Coulter DU730 spectrophotometer. For the assays with metal solutions, M9 medium was supplemented with one of the following metals: 100 μM $Al_2(SO_4)_3$, 20 μM $CuSO_4$, 30 μM $NiCl_2$, 30 μM $MnCl_2$, or 30 μM $FeSO_4$. All chemicals were purchased from Sigma-Aldrich (St. Louis, MO, USA).

Selection of H_2O_2-tolerant clones. A 2% inoculum of a coexisting frozen dual-plasmid library stock was cultured in 125 ml LB medium in a baffled flask to an OD_{600} of 1. The cells were diluted in a 1:10 ratio into 20 ml of prewarmed LB medium, and H_2O_2 was added to a final concentration of 14 mM. Cultures were incubated at 37°C for 30 min. The concentration of H_2O_2 and the stress exposure time were selected based on preliminary experiments to obtain a survival rate of approximately 0.05%, which allows the elimination of false-positive results. Dilutions of the surviving cells were plated, and surviving clones were selected. Plasmids from the strains exhibiting a better survival rate (than the control) were isolated and sequenced. These plasmids were also retransformed into *E. coli* K-12 strain MG1655 to make sure that the H_2O_2 tolerance was not from any possible chromosomal DNA mutations. Strains harboring the identified plasmids were evaluated with the oxidative stress resistance assay.

Plasmid construction. Plasmid pLib identified in this study includes the genes *cueR*, *ybbJ*, *qmcA*, *fetA* (formerly *ybbL*), and *fetB* (formerly *ybbM*) and an incomplete *ybbN* gene. Four plasmids were constructed with genomic fragments that included different genes from pLib (pF1 to pF4) (Fig. 1C). The operon structure of *fetA* and *fetB* was maintained, and native promoters were used for expression of all genes. *E. coli* MG1655 genomic DNA was used for all PCRs, and primers are listed in Table 1. Fragment 1 (pF1) was PCR amplified with primer set pLib-For and *ybbJ*-promoter. Fragment 2 (pF2) was PCR amplified with primers pLib-For and *qmcA*-promoter. Fragments 3 (pF3) and 4 (pF4) were PCR amplified with primer pLib-intergenic and *fetB*-Rev or pLibRev, respectively. PCR products were adenylated, cloned into pCR8/GW/TOPO (Invitrogen, Carlsbad, CA, USA), and shuffled via an LR recombination reaction into pDEST14 (Invitrogen), according to the manufacturer's protocols. Plasmid pUC-GFP was previously constructed by amplifying the green fluorescent protein gene (*gfp*) from pLenti7.3/V5-GW/lacZ (Invitrogen, Carlsbad, CA) with primers GFP-for (GCATAGGATCCTTAAGAAGGA GAACCTAGCATGGTGAGCAAGGGCGA) and GFP-rev (TCCATG ACAGCAGGACCGAATTCAGGTACCTTACTTGTACAGCTCGT) and cloning the resulting fragment into pUC19 using the BamHI and EcoRI restriction sites. To construct plasmid pF3-GFP, primers GFP MfeI For and GFP MfeI Rev were used to amplify *gfp* from pUC-GFP so that it could be inserted into plasmid pF3 and replace the stop codon of FetB with the start codon of GFP, creating a FetB-GFP fusion. The resulting protein fusion utilizes the native *fetB* promoter and ribosomal binding site. Plasmids were confirmed by sequencing and transformed into BW25113 by electroporation.

H_2O_2 survival assay. Cultures were grown aerobically at 37°C with shaking at 220 rpm in standard LB or minimal M9 medium (29). Resistance to H_2O_2 stress was determined in cultures treated with H_2O_2 at 37°C for 30 min. A 1% inoculum of a culture grown overnight was grown to an OD_{600} of 1, diluted 10-fold in 5 ml of prewarmed medium, and stressed with 4 mM H_2O_2 at 37°C for 30 min. Cell survival was determined by dilution plate counts pre- and poststress. Survival was defined as follows: % survival = $[(CFU/ml)_{poststress}/(CFU/ml)_{prestress}] \times 100$. Higher H_2O_2 survival, and thus a more resistant strain, was defined as a higher percent survival than the appropriate control strain. For M9 minimal medium assays, cultures were grown to an OD_{600} of 0.5, and the assay was performed in a similar manner. For the assays with M9 minimal medium with metals, the metal was added to the desired concentration during cell growth and during the assay. For assays with BW25113 Δ*fur* strains, 250 U/ml catalase (CAT) was added to the medium for dilution series poststress to eliminate residual H_2O_2. Catalase was not added to other assay mixtures, since dilutions of $>10^3$ were performed prior to plating.

Quantitative (real-time) reverse transcription-PCR. RNA was isolated from *E. coli* BW25113 harboring plasmid pF3 (Fig. 1A) or the control plasmid at an OD_{600} of 1 by using the RNeasy kit (Qiagen). Reverse transcription for cDNA generation and quantitative (real-time) reverse transcription-PCR (Q-RT-PCR) for gene quantification were performed as described previously (30). The transcripts of *fetA* and *fetB* were quantitated by using *ihfB* as the housekeeping gene (31). Primer sequences are listed in Table 1. Expression ratios were determined by using Pfaffl equation 1 (32).

Enzyme assays for catalase and superoxide dismutase activity. Cells were grown in LB medium to an OD_{600} of 1, and 15 ml of cells was washed twice in cold 50 mM KP_i–0.1 mM EDTA. The cells were lysed with glass

TABLE 1 Strains, plasmids, and oligonucleotides used in this study

Strain, plasmid, or primer	Genotype or sequence[a]	Source or Reference	Strain or plasmid(s) constructed
E. coli strains			
K-12 MG1655	F$^-$ λ$^-$ *ilvG rfb-50 rph-1*	Laboratory stock	
Competent NEB 5-alpha	*fhuA2*Δ(*argF-lacZ*)*U169 phoA glnV44* ϕ80 Δ(*lacZ*)M15 *gyrA96 recA1 relA1 endA1 thi-1 hsdR17*	New England Biolabs	
C24MgL	*E. coli* K-12 MG1655 containing two compatible plasmid libraries	This study[b]	
BW25113	F$^-$ Δ(*araD-araB*)*567* Δ*lacZ4787*(::*rrnB3*) λ$^-$ *rph-1* Δ(*rhaD-rhaB*)*568 hsdR514*	CGSC	
Δ*cueR* (JW0476-1; CGSC 8628)	F$^-$ Δ(*araD-araB*)*567* Δ*lacZ4787*(::*rrnB3*) Δ*cueR770*::*kan* λ$^-$ *rph-1* Δ(*rhaD-rhaB*)*568 hsdR514*	27	
Δ*qmcA* (JW04781-1; CGSC 8629)	F$^-$ Δ(*araD-araB*)*567* Δ*lacZ4787*(::*rrnB3*) Δ*qmcA772*::*kan* λ$^-$ *rph-1* Δ(*rhaD-rhaB*)*568 hsdR514*	27	
Δ*ybbJ*	F$^-$ Δ(*araD-araB*)*567* Δ*lacZ4787*(::*rrnB3*) Δ*ybbJ*::*kan* λ$^-$ *rph-1* Δ(*rhaD-rhaB*)*568 hsdR514*	This study	
Δ*fetA* (formerly Δ*ybbL*) (JW0479-1; CGSC 8630)	F$^-$ Δ(*araD-araB*)*567* Δ*lacZ4787*(::*rrnB3*) Δ*ybbL773*::*kan* λ$^-$ *rph-1* Δ(*rhaD-rhaB*)*568 hsdR514*	27	
Δ*fetB* (formerly Δ*ybbM*) (JW5066-1; CGSC 11156)	F$^-$ Δ(*araD-araB*)*567* Δ*lacZ4787*(::*rrnB3*) Δ*ybbM774*::*kan* λ$^-$ *rph-1* Δ(*rhaD-rhaB*)*568 hsdR514*	27	
Δ*fur*	F$^-$ Δ(*araD-araB*)*567* Δ*lacZ4787*(::*rrnB3*) Δ*fur*::*kan* λ$^-$ *rph-1* Δ(*rhaD-rhaB*)*568 hsdR514*	This study	
Δ*fetB* Δ*fur*	F$^-$ Δ(*araD-araB*)*567* Δ*lacZ4787*(::*rrnB3*) Δ*fetB* λ$^-$ Δ*fur*::*kan rph-1* Δ(*rhaD-rhaB*)*568 hsdR514*	This study	
Plasmids			
pLib	pDEST14; Amp^r plasmid with the *E. coli* locus at bp 513076–517376 spanning *cueR*, *ybbJ*, *qmcA*, *ybbL*, *ybbM*, and the incomplete *ybbN*	This study	
pF1	*cueR* and *ybbJ* (bp 513076–514301) in pDEST14; Amp^r	This study	
pF2	*cueR*, *ybbJ*, and *qmcA* (bp 513076–515047) in pDEST14; Amp^r	This study	
pF3	*fetA* and *fetB* (formerly *ybbL* and *ybbM*, respectively) (bp 515000–516646) in pDEST14; Amp^r	This study	
pF4	*fetA*, *fetB*, and the incomplete *ybbN* (bp 515000–517376) in pDEST14; Amp^r	This study	
pF3-GFP	*fetA* and *fetB* fused with GFP in pDEST14; Amp^r	This study	
pUC-GFP	GFP in pUC19	Laboratory construct	
pCntl	Control plasmid with the promoterless *Arabidopsis thaliana* β-glucuronidase (*gus*) gene in pDEST14; Amp^r	25	
Primers			
*ybbJ*KOFOR	CCGAGCTGGTGAAAGACAGCGCCAACAAACGGACTCAGCCGTGTAGGCTGGAGCTGCTTC		Δ*ybbJ*
*ybbJ*KOREV	CGAAAATCTCTCCGGCTGCTGTCATCATCGGGCAGGGTGAATGGGAATTAGCCATGGTCC		Δ*ybbJ*
*ybbJ*KOconfirmFor	CCCTGGCGATGACAGCGCCGACT		Δ*ybbJ*
*ybbJ*KOconfirmRev	GCAGATCGGTTCCTCCAGTAACAGC		Δ*ybbJ*
FurKOFor	TTTTCTCGTTCAGGCTGGCTTATTTGCCTTCGTGCGCATGGTGTAGGCTGGAGCTGCTTC		Δ*fur*
FurKORev	CGCATGACTGATAACAATACCGCCCTAAAGAAAGCTGGCCATGGGAATTAGCCATGGTCC		Δ*fur*
FurKOconfirmFor	CTCTCGCTTTTCTTATTTCCCTTGC		Δ*fur*
FurKOconfirmRev	TCAAGAGCAAATTCTGTCACTTCTT		Δ*fur*
pLib-For	CGCAATAAAACCGTATAACATCTCT		pF1, pF2
ybbJ-promoter	TTTTTACAGGCTGAAGCGCGTGAAC		pF1
qmcA-promoter	ATAATTTGTTTAATCAAGCAGCAAT		pF2
pLib-intergenic	GGAAAAACCTCCTGTTGTACCGTC		pF3, pF4
ybbM-Rev	TCCGTTGATCGGCACATGAACCAC		pF3
pLib-Rev	CAATTCTGGAAAGCCTCGCGGCGC		pF4
GFP MfeI For	AAGTCAATTGAAGAAGAAAATGGTGAGCAAGGGCGAGGAGCTGTTCACCGGGGT		pF3-GFP
GFP MfeI Rev	GGACCAATTGTTACTTGTACAGCTCGTCCATGCCGAGAGTGATCCCGGCG		pF3-GFP
fetA q-RT-PCR For	TATCTGGCGGGTGATGCGAAGAT		
fetA q-RT-PCR Rev	AAACAGTAACGTTCCGCTGGTTGG		
fetB q-RT-PCR For	ATCTGCTTTAATGCGGCGTGGAAC		
fetB q-RT-PCR Rev	AGGGATCACCTGCATCGGGATAAA		
ihfB q-RT-PCR For	AAGAGATGCTGGAGCATATGGCCT		
ihfB q-RT-PCR Rev	TGCAAAGAGAAACTGCCGAAACCG		

[a] Underlining in a primer sequence indicates the restriction endonuclease cut site.
[b] Using genomic libraries from reference 25.

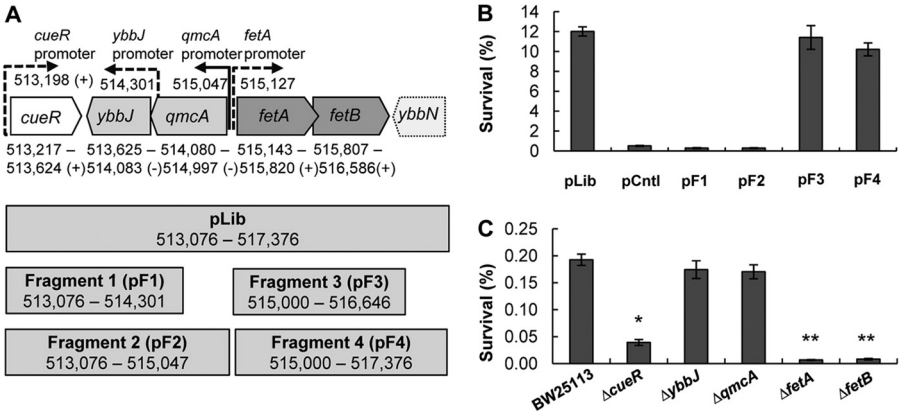

FIG 1 Role of the *E. coli* locus at positions 513217 to 517376 in H_2O_2 tolerance. (A, top) Genes included in plasmid pLib that enhances resistance to H_2O_2. pLib spans chromosomal positions 513217 to 517376 and includes the complete open reading frames of *cueR*, *ybbJ*, *qmcA*, *fetA* (*ybbL*), and *fetB* (*ybbM*) (solid lines) as well as the incomplete *ybbN* gene (dashed lines). Gene orientations and promoters (solid for experimental and dashed for predicted) were obtained from EcoCyc (45). (Bottom) Four fragments were cloned into plasmids pF1 to pF4 based on the sequence included in pLib. (B) Survival rates of *E. coli* BW25113 with plasmids pF1 to pF4 after a 30-min exposure to 4 mM H_2O_2 at 37°C. Cultures were grown to an OD_{600} of 1, diluted 10-fold in 5 ml of prewarmed LB medium, and stressed with H_2O_2 at 37°C for 30 min. Cell survival was determined by plating dilution series pre- and poststress as follows: % survival = $[(CFU/ml)_{poststress}/(CFU/ml)_{prestress}] \times 100$. pLib was the plasmid isolated during library enrichment. pF1, pF2, pF3, and pF4 are plasmids with inserts that correspond to fragments 1 to 4 illustrated in panel A. Data are means ± standard errors of the means ($n = 4$). (C) Rates of survival of *E. coli* strain BW25113 and the Δ*cueR*, Δ*ybbJ*, Δ*qmcA*, Δ*fetA*, and Δ*fetB* mutant strains against 4 mM H_2O_2 stress. Assays were performed as described above for panel B. Data are means ± standard errors of the means ($n = 3$). * indicates a statistical difference (P value of <0.05) for a Student t test performed between *E. coli* strain BW25113 and the Δ*cueR* strain. ** indicates a statistical difference (P value of <0.05) for a Student t test performed between the Δ*cueR* and the Δ*fetA* or Δ*fetB* strains.

beads (4 mg/ml) by vortexing for 1 min five times, with 1 min of resting on ice between cycles. Catalase activity was determined with an assay for H_2O_2 clearance, as described previously (33), with minor modifications. Fifty microliters of cell extract was diluted with 450 μl 50 mM KP_i (pH 7.0) with 10 mM H_2O_2. Aliquots were diluted 50-fold with 50 mM KP_i (pH 7.0) at 1-min intervals (33). The remaining H_2O_2 activity was determined by combining 400 μl of the sample with 800 μl of a colorimetric mixture composed of 1 mM KP_i (pH 7.0), 2.5 mM phenol, 0.5 mM 4-aminoantipyrine, 40 μg/ml horseradish peroxidase, and 500 nM H_2O_2 and measuring the absorbance at 505 nm (33, 34). Superoxide dismutase (SOD) activity was determined as detailed previously (35). The SOD assay is based on the competition for superoxide by the enzyme and cytochrome *c*, an indicator that undergoes a colorimetric change detectable at 505 nm. Superoxide was generated by the reaction of xanthine and xanthine oxidase. Units reported are standard McCord-Fridovich units (35). Protein was quantified by using the Bio-Rad RC DC protein assay kit. Three biological replicates were performed to determine the total catalase or SOD activity.

Bioinformatics analysis. Bioinformatics analysis of the sequences was performed by using BLAST (36). Multiple-sequence alignment was performed by using the ClustalW server (37, 38). The TMHMM v. 2.0 server was used to predict transmembrane domains and localization (39). The SMV-Prot server was used to further analyze protein function (40).

Microscopy sample preparation, instrumentation, and analysis. Superresolution structured illumination microscopy (SIM) was utilized for protein localization analysis (41). For microscopy, a 1% inoculum of culture was grown in LB medium at 25°C with shaking at 300 rpm for 6 h. Cells from 5 ml of culture were collected by centrifugation and resuspended in 1 ml 10 mM phosphate-buffered saline (PBS) (pH 7.4). Clean coverslips were covered in 0.05% poly-L-lysine for 30 min and rinsed with water. Cells (200 μl) were added onto the coverslips and allowed to settle for 30 min in the dark. Cells were then fixed with 2 ml of 4% paraformaldehyde in 10 mM PBS (pH 7.4) for 15 min in the dark. Cells were finally rinsed with PBS, and slides were prepared for microscopy using the fixed cells and 5 μl of SlowFade Gold Antifade reagent (Life Technologies). Superresolution SIM was performed with a Zeiss Elyra PS.1 microscope equipped with a Plan-Apochromat 63×/1.40 numerical aperture oil objective. Images were acquired with a 488-nm laser, a 495- to 550-nm-band-pass filter, a 28-μm grating period, and five SIM rotations. SIM reconstructions were conducted by using a theoretical point spread function and auto-noise feature with Zen 2012 software (Zeiss).

Electron paramagnetic resonance spectroscopy analysis. *E. coli* BW25113Δ*fur*(pF3) and BW25113Δ*fur*(pCntl) cultures were grown to an OD_{600} of 1 to 1.5 and were prepared for EPR spectroscopy analysis as described previously (42), with the modification that samples were washed in 20 mM Tris-HCl containing 50 mM EDTA. Samples (450 μl) were loaded into 4-mm thin-wall precision quartz EPR sample tubes (Wilmad, Vineland, NJ, USA) and analyzed on an a Bruker EMXmicro X-band spectrometer with a variable temperature unit (ER4141VT). The EPR spectrometer settings were as follows: 30.00 mW, with a microwave frequency of 9.37 GHz, modulation frequency of 100 kHz, modulation amplitude of 10.00 G, sweep rate of 4.88 G/s, and time constant of 81.92 ms. For protein quantification, 100 μl of sample was centrifuged, followed by resuspension of the pellet in 150 μl of 1× sodium dodecyl sulfate buffer, boiling for 5 min, and collection of the supernatant by centrifugation. The protein concentration was determined by using the Bio-Rad RC DC protein assay kit according to the manufacturer's instructions. The protein concentration was used to normalize the signal amplitude for the five biological replicates tested.

RESULTS

Overexpression of the *E. coli* genetic locus comprised of *cueR*, *ybbJ*, *qmcA*, *ybbL*, and *ybbM* increases resistance to H_2O_2-mediated stress. To identify genomic loci that impart resistance to H_2O_2 in *E. coli*, we screened two coexisting/coexpressing genomic libraries (CoGeLs) (25) for survival after a 30-min stress with 14 mM H_2O_2. Strains exhibiting a higher rate of survival against H_2O_2 were selected, and the two coexisting plasmids from these clones were isolated (see Table S1 in the supplemental material). The plasmids were retransformed into wild-type (WT) *E. coli* K-12 MG1655, and their tolerance to 4 mM H_2O_2 was examined. This was done to determine the role of each plasmid individually or together and, at the same time, guard against any potential

chromosomal mutations that might have occurred in the host during library screening. We found that a single plasmid, designated pLib, carrying a DNA fragment that includes the genes *cueR*, *ybbJ*, *qmcA*, *fetA* (formerly *ybbL*), and *fetB* (formerly *ybbM*) (Fig. 1A), was responsible for increased survival (Fig. 1B). These genes code for the CueR DNA-binding transcriptional regulator that is involved in copper resistance (43), the proteases YbbJ and QmcA (44), and the predicted ABC transporter proteins FetA (YbbL) and FetB (YbbM), which have not been characterized previously.

Overexpression of *fetA* and *fetB* increases survival under conditions of H_2O_2 stress. The genes of the DNA fragment in pLib were overexpressed in small subsets to determine which gene(s) is necessary for the improved tolerance to H_2O_2 stress. Four smaller fragments were generated, including the native promoters (Fig. 1A), and cloned into plasmids. The survival of strains harboring these fragments under conditions of oxidative stress was examined (Fig. 1B). pF3 (*fetA* and *fetB*) and pF4 (*fetA*, *fetB*, and part of *ybbN*) increased *E. coli* BW25113 survival under conditions of H_2O_2 stress to the levels observed with pLib, whereas *cueR*, *ybbJ*, and *qmcA* (pF1 and pF2) had no beneficial effect (Fig. 1B). pF3 contains the native promoters for transcription of *fetA* and *fetB*, and using Q-RT-PCR, we determined that the *fetA* and *fetB* transcript levels from pF3 increased by 49- and 35-fold, respectively, relative to those of the plasmid control. We conclude that *fetA* and *fetB* are the genes from pLib that, when overexpressed, impart a higher level of resistance to H_2O_2 stress.

Knockout mutants of *cueR*, *fetA*, and *fetB* exhibit increased sensitivity to H_2O_2 stress. The role of the pLib genes in oxidative stress resistance was also examined by using gene knockouts (KOs) in *E. coli* BW25113 (27). The BW23115 Δ*cueR*, Δ*qmcA*, Δ*fetA* (Δ*ybbL*), and Δ*fetB* (Δ*ybbM*) strains were obtained from the Keio Collection (27), and the BW23115 Δ*ybbJ* strain was generated by lambda red recombination (28). Survival of the strains with individual gene knockouts after 30 min of stress with 4 mM H_2O_2 at 37°C in LB medium was determined (Fig. 1C). The Δ*ybbJ* and Δ*qmcA* knockouts had survival rates similar to those of the wild type. Disruption of *cueR* decreased H_2O_2 survival by 79% compared to the wild type. The BW25113 Δ*fetA* and Δ*fetB* strains exhibited increased H_2O_2 sensitivity, with the poststress survival rate decreasing by >95% relative to the wild type. The Δ*fetA* and Δ*fetB* data corroborate the overexpression data (Fig. 1B). We conclude that *cueR*, *fetA*, and *fetB* have a role in oxidative stress resistance, whereby the deletion of these genes decreased survival against H_2O_2. However, since *cueR* overexpression in plasmids pF1 and pF2 did not increase tolerance to ROS (Fig. 1B), we focused on *fetA* and *fetB*, which increased survival under conditions of H_2O_2 stress.

To demonstrate complementation for the Δ*fetA* and Δ*fetB* strains, plasmid pF3 and a control plasmid were transformed into strain BW23115 and the BW23115 Δ*fetA* and Δ*fetB* knockout strains. With a control plasmid, the parent strain exhibited a higher survival rate than the knockouts (Fig. 2A). However, gene expression from pF3 increased survival against H_2O_2 for all strains (Fig. 2B). This demonstrates that complementation of the KO strains with pF3 restores the phenotype and abrogates H_2O_2 sensitivity (Fig. 2).

Bioinformatic analysis to determine the possible function of FetA and FetB. The identified genes, *fetA* and *fetB*, have not been previously studied; thus, we used bioinformatics to identify the possible role of these genes. EcoCyc suggests that FetA (YbbL) is

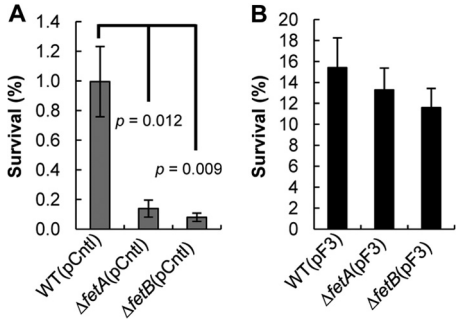

FIG 2 Complementation of Δ*fetA* and Δ*fetB* mutants with plasmid pF3 increases tolerance to H_2O_2 stress. Survival rates of *E. coli* BW25113 (WT) and the Δ*fetA* and Δ*fetB* strains with a control plasmid (pCntl) (A) or the *fetA* and *fetB* overexpression plasmid (pF3) (B) after 30 min of H_2O_2 stress were determined as described in the legend of Fig. 1B. Data are means ± standard errors of the means ($n = 5$). *P* values indicate the statistical significance of a Student *t* test performed between the WT and the KO strains.

an uncharacterized member of the ABC transporters and that FetB (YbbM) is a putative metal resistance inner membrane protein (45). BLASTp and multiple-sequence alignments showed that FetA contains the ABC transporter signature motif (LSGGEKQ RIS) flanked by the Walker A (P-loop) (GPSGCGKS) and Walker B (VLLLDE) motifs as well as the Q-loop, D-loop, and H-loop motifs, which are indicative of the ATP-binding cassettes (see Fig. S1A in the supplemental material) (46, 47). FetB belongs to the uncharacterized protein family UPF0014 (36). Analysis by the TMHMM v. 2.0 server predicts that FetB has seven transmembrane domains (see Fig. S1B in the supplemental material) (39). Analysis of FetB using the SMV-Prot server predicts that it belongs to the family of transmembrane proteins (*P* value, 98.6%), with a lower probability that it is an all-lipid-binding protein (*P* value, 90.3%), a sodium-binding protein (*P* value, 68.5%), a metal-binding protein (*P* value, 58.6%), or a secretory pathway protein (*P* value, 58.6%) (40). Combined, FetA and FetB are predicted to be an ABC-type transporter, with FetA being the ATP-binding component subunit and FetB being the inner membrane metal resistance protein.

To confirm that FetB is a membrane protein, we generated a GFP fusion by replacing the stop codon of FetB with the start codon of GFP in pF3 to generate plasmid pF3-GFP. In this construct, expression of GFP was driven by the native *fetB* promoter and ribosomal binding site. Superresolution structured illumination microscopy was used to compare the control strain (Fig. 3A), where GFP was not fused to FetB, to the strain harboring pF3-GFP, where the FetB-GFP fusion localizes in the membrane (Fig. 3B and C). These results illustrate that the FetB protein is expressed and is localized to the membrane, with the C-terminal GFP located in the cytoplasm.

FetB is well conserved among many *E. coli* strains, including *E. coli* W3110 and pathogenic *E. coli* O157:H7, as well as other *Enterobacteriaceae*, such as *Shigella dysenteriae* and *Salmonella enterica*. FetB is annotated as a putative metal resistance protein for *E. coli* O55:H7 RM12579, but the metal is unknown. FetB shares 37% homology with Star2 of *Oryza sativa japonica* (Japanese rice) and 35% homology with ALS3 of *Arabidopsis thaliana* (see Fig. S2 in the supplemental material), which have been described as ABC transport-like proteins that are involved in aluminum tolerance (48, 49). This information suggests that FetA and FetB constitute

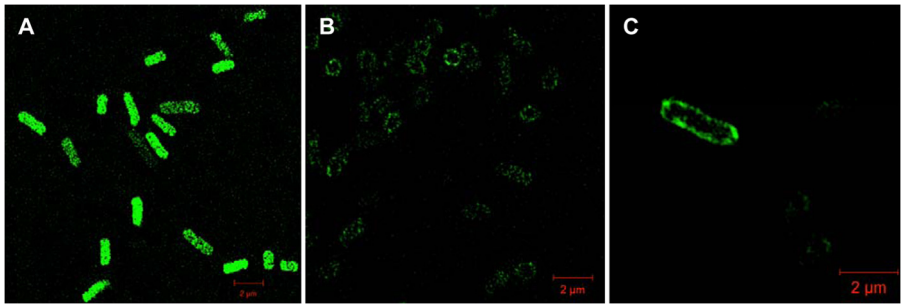

FIG 3 FetB localizes in the cell membrane, as determined by superresolution structured illumination microscopy. (A) The control, *E. coli* BW25113 with pUC-GFP, does not show localization of GFP, demonstrating that GFP is expressed throughout the cytoplasm. (B) *E. coli* BW25113 with pF3-GFP produces a fusion FetB-GFP protein that localizes in the cell membrane with the C-terminal GFP located in the cytoplasm. (*C*) A single *E. coli* cell with the FetB-GFP fusion localized in the membrane.

an ABC-type transporter that might facilitate the transport of aluminum or another metal.

The catalase and superoxide dismutase activities of *E. coli* are not affected by *fetA* and *fetB*. Bioinformatic analysis suggests that FetA and FetB constitute an ABC transporter involved in metal transport, but the physiological metal substrate and the mechanism of tolerance could not be determined. Metal transporters were previously shown to influence resistance to oxidative stress, as metal concentrations can influence the activity of catalases (CATs) and superoxide dismutases (SODs) (2, 50). In previous studies, knockout strains of ABC-type transporters exhibited decreased enzyme activity and increased sensitivity to oxidative stress (19, 51). To examine if the decreased H_2O_2 stress tolerance of the Δ*fetA* and Δ*fetB* strains was due to lower enzyme activities, we investigated the CAT and SOD activities of wild-type strain BW25113 and the Δ*fetA* and Δ*fetB* strains. The CAT and SOD activities of the Δ*fetA* and Δ*fetB* strains were not statistically different from those of the WT (Table 2). Thus, the lower rate of survival against H_2O_2 observed for these strains cannot be attributed to altered CAT or SOD activity.

Survival against H_2O_2-mediated stress is increased in minimal M9 medium. We next examined if tolerance to H_2O_2 stress due to *fetA* and *fetB* overexpression can be modified by the medium composition by performing survival assays with minimal M9 medium. We chose minimal M9 medium because it allows the control of metal concentrations by eliminating the variability from the undefined components of LB medium. In minimal medium, we observed the same trends, in terms of the H_2O_2 stress response, as those observed for the cultures grown in LB medium, whereby the Δ*fetA* and Δ*fetB* strains were more sensitive to oxidative stress than the WT strain (Fig. 4A). However, all strains had higher survival rates in M9 medium than in LB medium (Fig. 2), which suggests that LB medium contains components (most likely metal ions) that increase the sensitivity to oxidative stress. The survival rate of strain BW25113 with the control plasmid was 7.5% in M9 medium (Fig. 4A), compared to 1% in LB medium (Fig. 2A). The same trend was observed for the Δ*fetA* and Δ*fetB* strains. In M9 medium, the Δ*fetA* strain had a 1.67% survival rate, compared to 0.14% in LB medium. Similarly, the Δ*fetB* strain had a 1.21% survival rate in M9 medium, compared to 0.08% in LB

TABLE 2 Catalase and superoxide dismutase activities of WT BW25113 and the BW25113 Δ*fetA* and BW25113 Δ*fetB* strains[a]

Strain	Mean catalase activity (absorbance/min/mg protein) ± SEM	Mean superoxide dismutase activity (U/mg protein) ± SEM
BW25113	1.12 ± 0.31	73.6 ± 2.4
BW25113 Δ*fetA*	1.53 ± 0.52	89.0 ± 13.6
BW25113 Δ*fetB*	0.92 ± 0.22	58.2 ± 21.1

[a] Catalase activity was determined by H_2O_2 clearance as described previously (33), and superoxide dismutase activity was determined as detailed previously (35). The data from three biological replicates are reported.

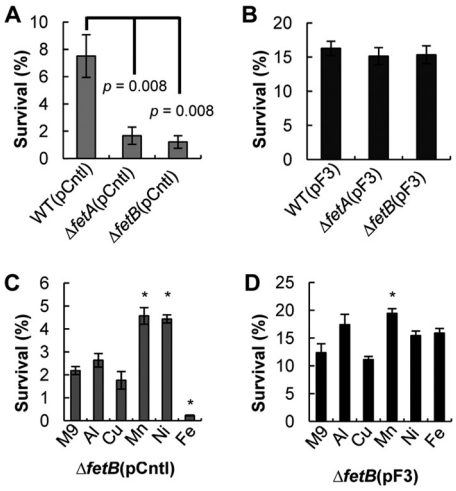

FIG 4 Characterization of strains in minimal M9 medium with and without added metals. (A) Survival rates of *E. coli* strain BW25113 (WT) and the Δ*fetA* and Δ*fetB* strains with a control plasmid after a 30-min exposure to 4 mM H_2O_2 at 37°C in M9 minimal medium. Data are means ± standard errors of the means ($n = 6$). *P* values indicate the statistical significance of a Student *t* test performed between the WT and the KO strains. (B) Survival rates of *E. coli* strain BW25113 (WT) and the Δ*fetA* and Δ*fetB* strains with plasmid pF3 after H_2O_2 stress. Data are means ± standard errors of the means ($n = 6$). (C) Survival of the BW25113 Δ*fetB* strain with a control plasmid (pCntl) under conditions of H_2O_2 stress in M9 minimal medium with different metals. Data are means ± standard errors of the means ($n = 3$). (D) Survival of the BW25113 Δ*fetB* strain with plasmid pF3 under conditions of H_2O_2 stress in M9 minimal medium with different metals. Data are means ± standard errors of the means ($n = 3$). For panels C and D, metals were added at the following concentrations: 100 μM $Al_2(SO_4)_3$, 20 μM $CuSO_4$, 30 μM $NiCl_2$, and 30 μM $FeSO_4$. Cultures were cultivated in the presence of metals and then stressed with 4 mM H_2O_2 for 30 min to determine survival. * represents a statistical difference, as determined by a Student *t* test, between the M9 and metal media (*P* value of <0.05).

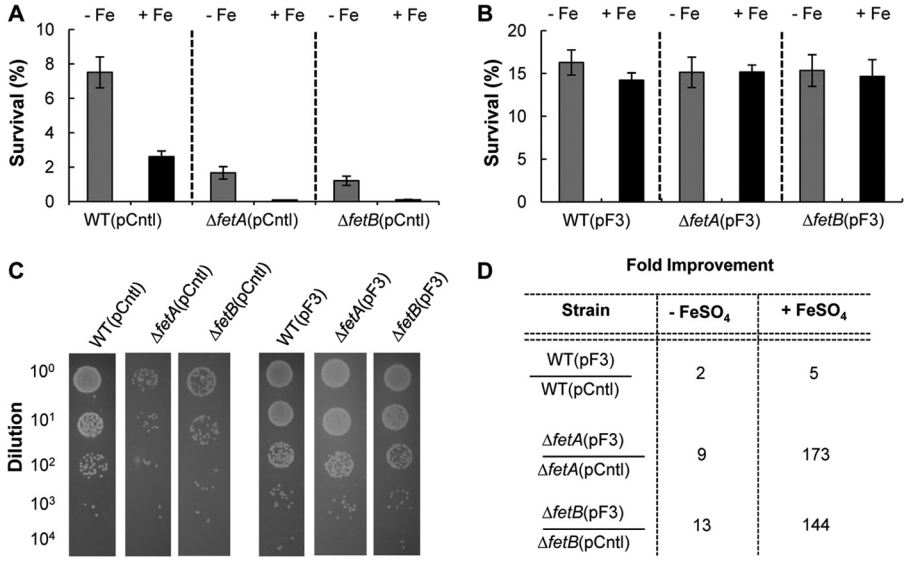

FIG 5 Survival against 4 mM H_2O_2 stress in M9 medium containing 30 μM $FeSO_4$. (A) *E. coli* strain BW25113 (WT) and the Δ*fetA* and Δ*fetB* strains with a control plasmid (pCntl) were grown in minimal medium in the presence (black bars) or absence (gray bars) of 30 μM $FeSO_4$. The cultures were stressed with 4 mM H_2O_2 at 37°C in M9 minimal medium with 30 μM $FeSO_4$ for 30 min, and survival rates were determined based on CFU. Data are means ± standard errors of the means ($n = 3$). (B) The strains with the pF3 overexpression plasmid were treated similarly to the strains described above for panel A. The survival rates of all overexpression strains are statistically indistinguishable. Data are means ± standard errors of the means ($n = 3$). (C) Final dilution series of assays performed with M9 medium with 30 μM $FeSO_4$ are shown for the pCntl strains (left) and the overexpression pF3 strains (right). For these assays, 10 μl of diluted culture poststress was spotted onto M9 agar plates and allowed to grow for 24 h. (D) The fold improvement of the different strains harboring the overexpression plasmid pF3 or pCntl was determined for assays in the presence or absence of $FeSO_4$.

medium. Since the knockout strains showed lower survival rates than the wild-type strain (Fig. 4A), but gene overexpression could still complement this defect (Fig. 4A and B), we conclude that the metal substrate of the FetA and FetB transporters should be one of the metal components in M9 minimal medium that is present in trace concentrations.

Overexpression of *fetA* and *fetB* increases survival under conditions of H_2O_2 stress in the presence of iron. Next, we screened various candidate metal substrates in M9 minimal medium, aiming to identify the substrate for FetA and FetB that is involved in oxidative stress damage. Aluminum [100 μM $Al_2(SO_4)_3$], copper (20 μM $CuSO_4$), nickel (30 μM $NiCl_2$), manganese (30 μM $MnCl_2$), and iron (30 μM $FeSO_4$) were added in minimal medium to investigate which metal is transported by FetA and FetB and can influence H_2O_2 stress survival. Aluminum was investigated due to the homology of FetB to Star2 and ALS3, which are involved in aluminum transport in plants (48, 49). Copper was chosen due to the proximity of *fetA* and *fetB* to *cueR* and *copA* in the *E. coli* chromosome, both of which are involved in copper resistance (52). The different metal concentrations were selected based on the toxicity of each metal, to ensure that growth prior to stress was not inhibited.

Initially, survival assays were performed on the Δ*fetB* strain with the overexpression (pF3) or control (pCntl) plasmid (Fig. 4C and D) to determine tolerance to H_2O_2 stress in the presence of different metals. For the Δ*fetB*(pCntl) strain, we observed an increase in survival in the presence of Mn or Ni, no significant change in the presence of Al or Cu, and a decrease in survival when iron was present (Fig. 4C).

The addition of iron greatly reduced the survival of the Δ*fetB*(pCntl) strain against H_2O_2 stress (Fig. 4C), suggesting that the knockout strain is unable to overcome iron overload coupled with oxidative stress. Is this increased H_2O_2 sensitivity due to iron, which can increase ROS through Fenton reactions, or due to the inability of the cells to cope with the excess metal? To address these questions, we studied the survival of the overexpression Δ*fetB*(pF3) strain in the presence of metals (Fig. 4D). Overexpression of *fetA* and *fetB* in the Δ*fetB* strain increased survival against H_2O_2 for all metals tested, and iron sensitivity was eliminated (Fig. 4D). This suggests that FetA and FetB have a role in iron homeostasis and that the decrease in the tolerance of the Δ*fetB* strain to H_2O_2 stress was due to its inability to cope with iron overload.

We next examined the survival rates of *E. coli* wild-type strain BW25113 and the BW25113 Δ*fetA* and BW25113 Δ*fetB* mutant strains under conditions of H_2O_2 stress in minimal medium in the presence and absence of iron to characterize all strains. The strains tested were more sensitive to H_2O_2 when iron was present, presumably due to the increased number of Fenton reactions, which result in higher ROS levels within the cells (Fig. 5A). However, the Δ*fetA* and Δ*fetB* strains were more severely impacted by iron than the parent *E. coli* strain BW25113 (Fig. 5A). Overexpression of *fetA* and *fetB* (plasmid pF3) increased resistance to H_2O_2 for all strains and abrogated the negative effect of iron (Fig. 5B). This suggests that FetA and FetB are able to regulate iron homeostasis and increase cell survival (Fig. 5C). The benefit of *fetA* and *fetB* overexpression in increasing survival against H_2O_2 stress was quantified. In the absence of iron, the survival rate of BW25113 increased 2-fold compared to that of the plasmid control strain (Fig. 5D). When iron was present, the survival rate of *E. coli* BW25113(pF3) increased 5-fold relative to that of control strain BW25113(pCntl) (Fig. 5D). The effects of *fetA* and *fetB* overexpression are evident in the Δ*fetA* and Δ*fetB* strains, where tolerance to oxidative stress was increased by a factor of 10 in minimal medium with no iron supplementation and was increased >100-

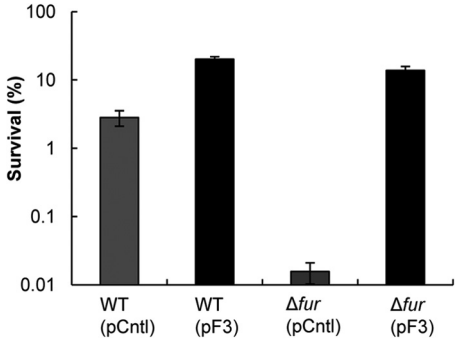

FIG 6 Survival of WT *E. coli* BW25113 and the Δ*fur* mutant under conditions of H_2O_2 stress in LB medium containing 30 μM $FeSO_4$. pCntl and pF3 descriptions are included in the legend of Fig. 1. The H_2O_2 stress assay was performed as described in the legend of Fig. 1, but the cultures were grown in medium containing 30 μM $FeSO_4$ to facilitate iron overload. Data are means ± standard errors of the means ($n = 5$).

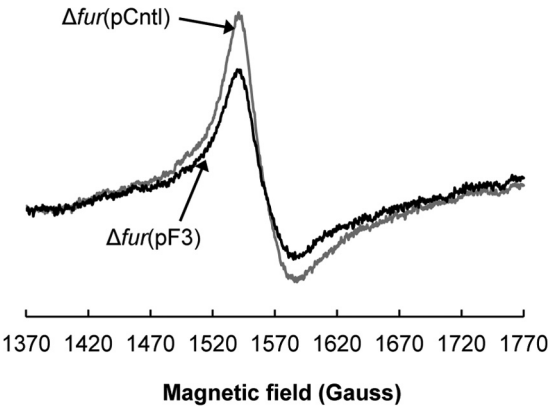

FIG 7 Overexpression of *fetA* and *fetB* in the *E. coli* BW25113 Δ*fur* strain decreases the overall intracellular free iron concentration, as determined by electron paramagnetic resonance (EPR). The BW25113 Δ*fur*(pF3) overexpression strain is shown in black, and the control Δ*fur*(pCntl) strain is shown in gray. Cultures grown aerobically in LB medium in exponential phase (OD_{600} of 1 to 2) were harvested and were oxidized with desferrioxamine mesylate as described previously (42). Samples loaded into 4-mm thin-wall precision quartz EPR sample tubes (Wilmad) were analyzed on a Bruker EMXmicro X-band spectrometer with a variable temperature unit (ER4141VT) with the following measurement settings: 30.00 mW, with microwave frequency of 9.37 GHz, a modulation frequency of 100 kHz, a modulation amplitude of 10.00 G, a sweep rate of 4.88 G/s, and a time constant of 81.92 ms. The signals were normalized by the protein concentration. Five biological replicates were analyzed, and data for a representative sample are shown.

fold when iron was added (Fig. 5D). Taken together, these data demonstrate that the FetA and FetB transporter has a role in iron homeostasis and increases H_2O_2 stress survival.

***fetA* and *fetB* overexpression guards against lethal oxidative damage in Δ*fur* mutants.** The Fur protein regulates iron uptake and superoxide dismutase expression (4), with *fur* mutants being unable to balance cellular iron content, thus resulting in iron overload (50). Iron accumulation in *fur* mutants results in severe oxidative damage and mutagenesis, with *fur recA* mutants being unable to survive under aerobic conditions (50). To investigate if overexpression of *fetA* and *fetB* could minimize iron overload in *fur* mutants, we constructed the BW25113 Δ*fur* and Δ*fur* Δ*fetB* strains and carried out H_2O_2 survival assays in the presence of 30 μM $FeSO_4$ in LB medium.

The BW25113 Δ*fur* and BW25113 Δ*fur* Δ*fetB* strains did not exhibit statistically different growth rates when cultured in LB medium with 100 μM $FeSO_4$ (see Fig. S3 in the supplemental material), indicating that iron overload alone is not sufficient for growth inhibition. However, the BW25113 Δ*fur* strain was more sensitive to oxidative damage than the parent BW25113 strain, as iron overload results in Fenton reactions that generate more ROS, resulting in cell death (see Fig. S4 in the supplemental material). As expected, the BW25113 Δ*fur* Δ*fetB* double mutant was extremely sensitive to H_2O_2, with the strain being unable to survive H_2O_2 stress under the assay conditions (see Fig. S4 in the supplemental material).

We next investigated if overexpression of *fetA* and *fetB* can overcome the deficiencies of the Δ*fur* strain. Survival of the Δ*fur*(pF3) strain increased in the presence of 30 μM $FeSO_4$ (Fig. 6), demonstrating that FetA and FetB have a role in overcoming the iron overload elicited by the *fur* mutation. This result corroborates data described above (Fig. 5), where we demonstrate that *fetA* and *fetB* overexpression can abrogate the negative effects of iron overload coupled with H_2O_2 stress. Furthermore, this finding suggests that the FetA and FetB transporter is not regulated by Fur directly. The Fur consensus sequence is not found upstream of *fetA* and *fetB* (53), suggesting that the transporter is regulated by other means.

Overexpression of *fetA* and *fetB* decreases intracellular iron levels in the Δ*fur* strain. The iron content in the BW25113 Δ*fur* strain was investigated by electron paramagnetic resonance (EPR), as deregulation of Fur results in iron overload. Samples from cultures grown aerobically in LB medium to exponential phase were prepared and analyzed by EPR. The total intracellular free iron content of the Δ*fur* strain with *fetA* and *fetB* overexpression was lower than that of the control strain (Fig. 7). The peak-to-peak amplitudes of five biological samples for the Δ*fur*(pF3) and Δ*fur*(pCntl) strains were compared by a *t* test (*P* value of 0.030), and the amplitude difference between the overexpression and control strains decreased by 37%. The Δ*fur* strains were still overloaded with iron, but overexpression of *fetA* and *fetB* resulted in lower cellular iron contents. Because ABC-type transporters operate between the cytoplasm and the periplasm, FetAB would export iron from the cytoplasm to the periplasm, where it can still be detected by whole-cell EPR. The overall iron content of the cells would then not be expected to decrease dramatically. This would explain why the amplitude of the signals for the Δ*fur*(pF3) strain are high even with *fetA* and *fetB* overexpression (Fig. 7). These EPR data indicate that FetA and FetB are involved in iron homeostasis and suggest that resistance to H_2O_2-mediated stress is increased by *fetA* and *fetB* overexpression due to decreased intracellular iron content, which results in fewer Fenton reactions and lower ROS formation rates.

DISCUSSION

In this study, we identified a genomic fragment spanning the *E. coli* genes *cueR*, *ybbJ*, *qmcA*, *fetA*, and *fetB* that enhances resistance to H_2O_2-mediated oxidative stress by screening genomic libraries. The genes included in the fragment were cloned in smaller subsets, and our results demonstrate that *fetA* and *fetB* overexpression can increase tolerance to oxidative stress. Gene knockouts were investigated, and we show that the deletion of *cueR*, *fetA*, or *fetB* results in increased sensitivity to H_2O_2 stress. The role of *cueR* in H_2O_2

stress can be attributed to the fact that CueR is a MerR family regulator that controls the expression of the copper efflux protein CopA (21, 52). The disruption of *cueR* results in the loss of *copA* expression (52), leading to increased copper overload and sensitivity. Copper targets iron-sulfur clusters, displacing and releasing iron (6), which, when coupled with H_2O_2 stress, can result in more ROS species being generated by Fenton reactions. This might explain why the deregulation of copper homeostasis in the Δ*cueR* strain renders *E. coli* more sensitive to H_2O_2 stress. Overexpression of *cueR* did not enhance tolerance to H_2O_2-mediated oxidative stress, and so we focused on better understanding the role of *ybbL* and *ybbM* in the observed phenotype.

The previously uncharacterized genes *fetA* and *fetB* are predicted to encode an ABC-type transporter that has a role in metal resistance. Metals can influence the activity of superoxide dismutase (SOD) (4), which catalyzes the removal of superoxide radicals, and thus have a role in oxidative stress tolerance. For example, a homologue of *Salmonella enterica* SitABCD was shown to transport Mn and Fe in *E. coli* and increase resistance to H_2O_2 (20). Similarly, the MtsABC transporter for Mn and Fe in *Streptococcus pyogenes* was implicated in oxidative stress resistance, and the MtsABC mutant was shown to have reduced SOD activity, attributed to lower intracellular Mn levels (19). We investigated both the SOD and catalase activities of the Δ*fetA* and Δ*fetB* strains to investigate if the lower levels of H_2O_2 tolerance of these strains can be attributed to a change in enzymatic activity. The knockout strains had activities similar to those of the wild-type strain, suggesting that the observed changes in tolerance are not due to a change in enzyme activity but are due to another mechanism.

We demonstrate that FetB is indeed a membrane protein, and we hypothesized that FetA and FetB allow for the transport of a metal that is involved in H_2O_2 resistance. For a metal that promotes oxidative stress, such as Fe, import should decrease tolerance to H_2O_2 stress, whereas export should increase survival by eliminating the metal. Conversely, if the metal has a beneficial effect on tolerance to ROS such as Mn, import should increase survival against H_2O_2 stress, and metal export should decrease tolerance. We performed H_2O_2-mediated stress assays in cultures grown in medium containing Al, Cu, Ni, Mn, or Fe.

Mn and Ni increased resistance to H_2O_2 stress, but these metals cannot be transported by FetA and FetB, since these assays were performed with the Δ*fetB* strain, suggesting that the beneficial effect is due to the metals and not due to the transporter. It is established that manganese can have a protective effect against oxidative stress by substituting for iron in different enzymes, thus minimizing Fenton reactions, and by being a cofactor for manganese-SOD (5, 19). The protective mechanism of Mn is supported by our data, which show that Mn increases tolerance to H_2O_2 stress for BW25113 and the Δ*fetA* and Δ*fetB* mutant strains (see Fig. S5A and S5B in the supplemental material). Therefore, manganese provides a protective effect against H_2O_2 regardless of FetAB.

Iron had a detrimental effect on oxidative stress tolerance in the absence of the ABC-type transporter in the Δ*fetB* strain. The lower survival rate is presumably due to Fenton reactions that produce more ROS. The overexpression of *fetA* and *fetB* increased tolerance to H_2O_2-mediated stress in the presence of iron, suggesting that the ABC-type transporter has a role in iron homeostasis. The BW25113 Δ*fur* strain, where the iron regulator is deleted, rendering strains unable to survive H_2O_2 stress in the presence of iron, was used to show that *fetA* and *fetB* overexpression can increase tolerance under conditions of iron overload. Furthermore, whole-cell EPR revealed a lower intracellular iron content in Δ*fur* strains in the presence of *fetA* and *fetB*. Combined, these data suggest that the ABC-type transporter has a role in iron homeostasis and increases H_2O_2 stress tolerance. It is possible that FetA and FetB function via another mechanism, such as a the metalation of a secreted protein to minimize oxidative stress, but the data presented here provide a strong link to iron transport.

This study is the first to reveal that overexpression of *fetA* and *fetB* increases H_2O_2 stress tolerance in *E. coli* and to experimentally demonstrate that FetB is a membrane protein. To explain the enhancement in oxidative stress survival, we put forward the hypothesis that the ABC-type transporter FetAB allows for iron homeostasis, thereby reducing Fenton reactions generated by H_2O_2. We provide evidence to link these genes and their products to iron transport, but the exact mechanism of transport remains unclear and will require further investigation. This is just one possible explanation, and further studies will need to be performed to fully validate our hypothesis. However, the improved phenotype, namely, the increased resistance to oxidative stress due to *fetA* and *fetB* overexpression, can be utilized to increase the efficiency of *E. coli* production systems in situations where oxidative stress arises.

ACKNOWLEDGMENTS

We thank Hongzhan Huang (University of Delaware) for helpful insights and assistance in utilizing bioinformatics tools for protein analysis. We thank the Yale *E. coli* genetic resources and the Coli Genetic Stock Center (CGSC) for supplying the Keio Collection strains. We are grateful to Stefan Gaida for providing the pUC-GFP vector used in the microscopy work. We also extend our gratitude to Jeffrey Caplan of the Delaware Biotechnology Institute Bioimaging Center for assistance with superresolution structured illumination microscopy and analysis.

This work was supported by National Science Foundation grant CBET-1033926 and Office of Naval Research (USA) grant N000141010161.

REFERENCES

1. **Aussel L, Zhao WD, Hebrard M, Guilhon AA, Viala JPM, Henri S, Chasson L, Gorvel JP, Barras F, Meresse S.** 2011. Salmonella detoxifying enzymes are sufficient to cope with the host oxidative burst. Mol. Microbiol. **80:**628–640.
2. **Imlay JA.** 2008. Cellular defenses against superoxide and hydrogen peroxide. Annu. Rev. Biochem. **77:**755–776.
3. **Liu YY, Bauer SC, Imlay JA.** 2011. The YaaA protein of the Escherichia coli OxyR regulon lessens hydrogen peroxide toxicity by diminishing the amount of intracellular unincorporated iron. J. Bacteriol. **193:**2186–2196.
4. **Andrews SC, Robinson AK, Rodriguez-Quinones F.** 2003. Bacterial iron homeostasis. FEMS Microbiol. Rev. **27:**215–237.
5. **Anjem A, Varghese S, Imlay JA.** 2009. Manganese import is a key element of the OxyR response to hydrogen peroxide in Escherichia coli. Mol. Microbiol. **72:**844–858.
6. **Macomber L, Imlay JA.** 2009. The iron-sulfur clusters of dehydratases are primary intracellular targets of copper toxicity. Proc. Natl. Acad. Sci. U. S. A. **106:**8344–8349.
7. **Xu FF, Imlay JA.** 2012. Silver(I), mercury(II), cadmium(II), and zinc(II) target exposed enzymic iron-sulfur clusters when they toxify Escherichia coli. Appl. Environ. Microbiol. **78:**3614–3621.
8. **Basak S, Jiang R.** 2012. Enhancing E. coli tolerance towards oxidative stress via engineering its global regulator cAMP receptor protein (CRP). PLoS One **7:**e51179. doi:10.1371/journal.pone.0051179.
9. **Nicolaou SA, Gaida SM, Papoutsakis ET.** 2010. A comparative view of metabolite and substrate stress and tolerance in microbial bioprocessing: from biofuels and chemicals, to biocatalysis and bioremediation. Metab. Eng. **12:**307–331.
10. **Keyer K, Imlay JA.** 1996. Superoxide accelerates DNA damage by elevating free-iron levels. Proc. Natl. Acad. Sci. U. S. A. **93:**13635–13640.

11. **Almiron M, Link AJ, Furlong D, Kolter R.** 1992. A novel DNA-binding protein with regulatory and protective roles in starved Escherichia coli. Genes Dev. **6:**2646–2654.
12. **Krewulak KD, Vogel HJ.** 2008. Structural biology of bacterial iron uptake. Biochim. Biophys. Acta **1778:**1781–1804.
13. **Marlovits TC, Haase W, Herrmann C, Aller SG, Unger VM.** 2002. The membrane protein FeoB contains an intramolecular G protein essential for Fe(II) uptake in bacteria. Proc. Natl. Acad. Sci. U. S. A. **99:**16243–16248.
14. **McHugh JP, Rodriguez-Quinones F, Abdul-Tehrani H, Svistunenko DA, Poole RK, Cooper CE, Andrews SC.** 2003. Global iron-dependent gene regulation in Escherichia coli—a new mechanism for iron homeostasis. J. Biol. Chem. **278:**29478–29486.
15. **Baumler AJ, Norris TL, Lasco T, Voigt W, Reissbrodt R, Rabsch W, Heffron F.** 1998. IroN, a novel outer membrane siderophore receptor characteristic of Salmonella enterica. J. Bacteriol. **180:**1446–1453.
16. **Salvail H, Lanthier-Bourbonnais P, Sobota JM, Caza M, Benjamin JAM, Mendieta MES, Lepine F, Dozois CM, Imlay J, Masse E.** 2010. A small RNA promotes siderophore production through transcriptional and metabolic remodeling. Proc. Natl. Acad. Sci. U. S. A. **107:**15223–15228.
17. **Thompson MG, Corey BW, Si YZ, Craft DW, Zurawski DV.** 2012. Antibacterial activities of iron chelators against common nosocomial pathogens. Antimicrob. Agents Chemother. **56:**5419–5421.
18. **Lewis VG, Ween MP, McDevitt CA.** 2012. The role of ATP-binding cassette transporters in bacterial pathogenicity. Protoplasma **249:**919–942.
19. **Janulczyk R, Ricci S, Bjorck L.** 2003. MtsABC is important for manganese and iron transport, oxidative stress resistance, and virulence of Streptococcus pyogenes. Infect. Immun. **71:**2656–2664.
20. **Sabri M, Leveille S, Dozois CM.** 2006. A SitABCD homologue from an avian pathogenic Escherichia coli strain mediates transport of iron and manganese and resistance to hydrogen peroxide. Microbiology **152:**745–758.
21. **Rensing C, Fan B, Sharma R, Mitra B, Rosen BP.** 2000. CopA: an Escherichia coli Cu(I)-translocating P-type ATPase. Proc. Natl. Acad. Sci. U. S. A. **97:**652–656.
22. **Rensing C, Mitra B, Rosen BP.** 1997. The zntA gene of Escherichia coli encodes a Zn(II)-translocating P-type ATPase. Proc. Natl. Acad. Sci. U. S. A. **94:**14326–14331.
23. **Grass G, Otto M, Fricke B, Haney CJ, Rensing C, Nies DH, Munkelt D.** 2005. FieF (YiiP) from Escherichia coli mediates decreased cellular accumulation of iron and relieves iron stress. Arch. Microbiol. **183:**9–18.
24. **Grass G.** 2006. Iron transport in Escherichia coli: all has not been said and done. Biometals **19:**159–172.
25. **Nicolaou SA, Gaida SM, Papoutsakis ET.** 2011. Coexisting/coexpressing genomic libraries (CoGeL) identify interactions among distantly located genetic loci for developing complex microbial phenotypes. Nucleic Acids Res. **39:**e152. doi:10.1093/nar/gkr817.
26. **Nicolaou SA, Gaida SM, Papoutsakis ET.** 2012. Exploring the combinatorial genomic space in Escherichia coli for ethanol tolerance. Biotechnol. J. **7:**1337–1345.
27. **Baba T, Ara T, Hasegawa M, Takai Y, Okumura Y, Baba M, Datsenko KA, Tomita M, Wanner BL, Mori H.** 2006. Construction of Escherichia coli K-12 in-frame, single-gene knockout mutants: the Keio Collection. Mol. Syst. Biol. **2:**2006.0008. doi:10.1038/msb4100050.
28. **Datsenko KA, Wanner BL.** 2000. One-step inactivation of chromosomal genes in Escherichia coli K-12 using PCR products. Proc. Natl. Acad. Sci. U. S. A. **97:**6640–6645.
29. **Sambrook J, Russell DW.** 2001. Molecular cloning: a laboratory manual, 3rd ed. Cold Spring Harbor Laboratory Press, Cold Spring Harbor, NY.
30. **Borden JR, Jones SW, Indurthi D, Chen YL, Papoutsakis ET.** 2010. A genomic-library based discovery of a novel, possibly synthetic, acid-tolerance mechanism in Clostridium acetobutylicum involving noncoding RNAs and ribosomal RNA processing. Metab. Eng. **12:**268–281.
31. **Zhou K, Zhou L, Lim Q, Zou R, Stephanopoulos G, Too HP.** 2011. Novel reference genes for quantifying transcriptional responses of Escherichia coli to protein overexpression by quantitative PCR. BMC Mol. Biol. **12:**18. doi:10.1186/1471-2199-12-18.
32. **Pfaffl MW.** 2001. A new mathematical model for relative quantification in real-time RT-PCR. Nucleic Acids Res. **29:**e45. doi:10.1093/nar/29.9.e45.
33. **Macomber L, Rensing C, Imlay JA.** 2007. Intracellular copper does not catalyze the formation of oxidative DNA damage in Escherichia coli. J. Bacteriol. **189:**1616–1626.
34. **Green MJ, Hill HAO.** 1984. Chemistry of dioxygen. Methods Enzymol. **105:**3–22.
35. **McCord JM.** 2001. Analysis of superoxide dismutase activity, p 7.3.1–7.3.9. *In* Maines MD (ed), Current protocols in toxicology. John Wiley & Sons, Inc., New York, NY.
36. **Altschul SF, Madden TL, Schaffer AA, Zhang JH, Zhang Z, Miller W, Lipman DJ.** 1997. Gapped BLAST and PSI-BLAST: a new generation of protein database search programs. Nucleic Acids Res. **25:**3389–3402.
37. **Goujon M, McWilliam H, Li WZ, Valentin F, Squizzato S, Paern J, Lopez R.** 2010. A new bioinformatics analysis tools framework at EMBL-EBI. Nucleic Acids Res. **38:**W695–W699. doi:10.1093/nar/gkq313.
38. **Larkin MA, Blackshields G, Brown NP, Chenna R, McGettigan PA, McWilliam H, Valentin F, Wallace IM, Wilm A, Lopez R, Thompson JD, Gibson TJ, Higgins DG.** 2007. Clustal W and Clustal X version 2.0. Bioinformatics **23:**2947–2948.
39. **Krogh A, Larsson B, von Heijne G, Sonnhammer ELL.** 2001. Predicting transmembrane protein topology with a hidden Markov model: application to complete genomes. J. Mol. Biol. **305:**567–580.
40. **Cai CZ, Han LY, Ji ZL, Chen X, Chen YZ.** 2003. SVM-Prot: Web-based support vector machine software for functional classification of a protein from its primary sequence. Nucleic Acids Res. **31:**3692–3697.
41. **Gustafsson MGL.** 2000. Surpassing the lateral resolution limit by a factor of two using structured illumination microscopy. J. Microsc. **198:**82–87.
42. **Woodmansee AN, Imlay JA.** 2002. Quantitation of intracellular free iron by electron paramagnetic resonance spectroscopy. Methods Enzymol. **349:**3–9.
43. **Yamamoto K, Ishihama A.** 2005. Transcriptional response of Escherichia coli to external copper. Mol. Microbiol. **56:**215–227.
44. **Chiba S, Ito K, Akiyama Y.** 2006. The Escherichia coli plasma membrane contains two PHB (prohibitin homology) domain protein complexes of opposite orientations. Mol. Microbiol. **60:**448–457.
45. **Keseler IM, Collado-Vides J, Santos-Zavaleta A, Peralta-Gil M, Gama-Castro S, Muniz-Rascado L, Bonavides-Martinez C, Paley S, Krummenacker M, Altman T, Kaipa P, Spaulding A, Pacheco J, Latendresse M, Fulcher C, Sarker M, Shearer AG, Mackie A, Paulsen I, Gunsalus RP, Karp PD.** 2011. EcoCyc: a comprehensive database of Escherichia coli biology. Nucleic Acids Res. **39:**D583–D590. doi:10.1093/nar/gkq1143.
46. **Linton KJ, Higgins CF.** 1998. The Escherichia coli ATP-binding cassette (ABC) proteins. Mol. Microbiol. **28:**5–13.
47. **Walker JE, Saraste M, Runswick MJ, Gay NJ.** 1982. Distantly related sequences in the alpha-subunits and beta-subunits of ATP synthase, myosin, kinases and other ATP-requiring enzymes and a common nucleotide binding fold. EMBO J. **1:**945–951.
48. **Huang CF, Yamaji N, Mitani N, Yano M, Nagamura Y, Ma JF.** 2009. A bacterial-type ABC transporter is involved in aluminum tolerance in rice. Plant Cell **21:**655–667.
49. **Larsen PB, Geisler MJB, Jones CA, Williams KM, Cancel JD.** 2005. ALS3 encodes a phloem-localized ABC transporter-like protein that is required for aluminum tolerance in Arabidopsis. Plant J. **41:**353–363.
50. **Touati D, Jacques M, Tardat B, Bouchard L, Despied S.** 1995. Lethal oxidative damage and mutagenesis are generated by iron in delta fur mutants of Escherichia coli: protective role of superoxide dismutase. J. Bacteriol. **177:**2305–2314.
51. **Rong C, Zhang C, Zhang Y, Qi L, Yang J, Guan G, Li Y, Li J.** 2012. FeoB2 functions in magnetosome formation and oxidative stress protection in Magnetospirillum gryphiswaldense strain MSR-1. J. Bacteriol. **194:**3972–3976.
52. **Stoyanov JV, Hobman JL, Brown NL.** 2001. CueR (YbbI) of Escherichia coli is a MerR family regulator controlling expression of the copper exporter CopA. Mol. Microbiol. **39:**502–511.
53. **Lavrrar JL, Christoffersen CA, McIntosh MA.** 2002. Fur-DNA interactions at the bidirectional fepDGC-entS promoter region in Escherichia coli. J. Mol. Biol. **322:**983–995.